

A Novel *IGHMBP2* Missense Variant in an Iranian Family with CMT2S: Experimental and Computational Approaches

Morteza Karbasi and Masoud Garshasbi*

Department of Medical Genetics, Faculty of Medical Sciences, Tarbiat Modares University, Tehran, Iran

ARTICLE INFO

Article history:

Received 28 November 2025

Accepted 30 December 2025

Available 24 January 2026

Keywords:

Charcot-marie-tooth disease

CMT2S

Exome sequencing

IGHMBP2

Novel variant

Supplementary information:

Supplementary information for

this article is available at

<http://sc.journals.umz.ac.ir/>

*Corresponding authors:

✉ M. Garshasbi

masoud.garshasbi@modares.ac.ir

p-ISSN 2423-4257

e-ISSN 2588-2589

ABSTRACT

Variants in the immunoglobulin mu-binding protein 2 (*IGHMBP2*) gene are associated with two phenotypes: The first phenotype is spinal muscular atrophy with respiratory distress type 1 (SMARD1), an alpha motor neuron disorder characterized by diaphragmatic paralysis and early death, often within the first year of life. The second phenotype is Charcot-Marie-Tooth disease type 2S (CMT2S), a slowly progressive axonal neuropathy marked by sensory loss and typically lacking respiratory involvement. This study aimed to identify the genetic cause of CMT2S in an Iranian family and to review previously reported variants and clinical features of CMT2S in the literature. Exome sequencing was performed on the affected proband. The candidate variant was subsequently validated in additional family members using Sanger sequencing. The pathogenicity and novelty of the variant were assessed using *in silico* prediction tools and available databases. We identified a novel homozygous variant, c.509T>C (p. Leu170Pro), in the *IGHMBP2* gene. 60 patients (59 patients + 1 case) were analyzed with CMT2S in our literature review. The main symptoms observed among these patients included muscle weakness and atrophy, absent reflexes, foot deformities, and gait disturbances. Atypical symptoms, including respiratory problems, gastrointestinal disturbances, and bladder dysfunction, were reported in a minority of cases. Among patients with an available age of onset, the mean age was 3.40 (SD± 3.83 years), with an interquartile range of 4.33 years. Across the analyzed patients, 98 total variants were included in the final mutational spectrum. Among these variants, c.1235+3A>G (p.Ala355Leufs*10) was the most frequently reported variant, occurring in seven patients. We report the second known case of CMT2S in a patient of Iranian descent, associated with a novel biallelic variant in the *IGHMBP2* gene. Our findings, along with previous findings from the literature, expand the mutational spectrum of *IGHMBP2* in CMT2S, contributing to a better understanding of its clinical and genetic heterogeneity.

© 2026 University of Mazandaran

Please cite this paper as: Karbasi, M., & Garshasbi, M. (2026). A Novel *IGHMBP2* missense variant in an Iranian family with CMT2S: experimental and computational approaches. *Journal of Genetic Resources*, 12(1), 94-106. doi: [10.22080/jgr.2026.31751.1462](https://doi.org/10.22080/jgr.2026.31751.1462)

Introduction

The *IGHMBP2* gene (OMIM: 600502), located on chromosome 11q13.3, has 15 exons and encodes a 993-amino-acid protein. The *IGHMBP2* protein—also known as SMUBP2, cardiac transcription factor 1, and glial factor 1—is a member of the UPF1-like group within the helicase superfamily 1. It functions as an ATP-dependent helicase that unwinds DNA and RNA duplexes and plays key roles in mRNA transcription, translation, and

RNA decay (De Planell-Saguer *et al.*, 2009; Kanaan *et al.*, 2018; Park *et al.*, 2024). This protein consists of three main domains: a helicase domain, an R3H domain, and an AN1-type zinc finger motif. The helicase domain contains two RecA-like subdomains (1A and 2A), and two accessory subdomains (1B and 1C) within RecA-1A, which all contribute to the binding of single-stranded RNA. Helicase processivity is regulated by the subdomains 1B and 1C (Kanaan *et al.*,



2018). The C-terminal domains, including the R3H domain and zinc finger motif, recognize the phosphorylated 5' end of single-stranded DNA, enhancing the ATPase activity of the helicase core and facilitating RNA and ribosomal binding (Lim *et al.*, 2012; Prusty *et al.*, 2024).

Until now, variants in *IGHMBP2* have been linked to CMT2S and SMARD1. SMARD1, caused by alpha motor neuron degeneration, is characterized by respiratory distress at an early stage, which leads to mechanical ventilation between six weeks and six months of age and muscular atrophy of distal limbs in the first years of life. In contrast, CMT2S presents a milder, chronic phenotype marked by motor and sensory impairment in the distal limbs, often without respiratory involvement (Cottenie *et al.*, 2014). About 71% of the variants were attributed to SMARD1, and only 29% to CMT2S. The pathomechanism of how *IGHMBP2* variants cause these disorders is not fully understood (Rzepnikowska *et al.*, 2024; Rzepnikowska and Kochanski, 2021; Tian *et al.*, 2023).

In this study, we present a novel *IGHMBP2* variant identified in a patient diagnosed with CMT2S. This case represents the second reported patient of Iranian descent. We performed bioinformatics analysis, protein modeling, a co-segregation study, and an evaluation of evolutionary conservation to assess the potential impact of the variant. Additionally, we provide a comprehensive review of the existing literature on this condition.

Materials and Methods

DNA extraction and whole-exome sequencing

The extraction of genomic DNA from patients' blood samples was accomplished using the salting-out method. The quality and quantity of the extracted DNA were evaluated using a Nanodrop spectrophotometer and gel electrophoresis. Exome enrichment was performed using the Twist Human Core Exome Kit, and the prepared library was sequenced on the Illumina NovaSeq 6000 platform (Illumina, Inc., San Diego, CA, USA).

Bioinformatic analysis

FastQC was used to assess the quality of the FASTQ files. We also used Trimmomatic to eliminate low-quality reads and adapter

sequences (Bolger *et al.*, 2014). Following quality control, the clean reads were aligned to the reference genome GRCh38/hg38 using the Burrows-Wheeler Aligner. Variant calling was conducted using the Haplotype Caller module of the Genome Analysis Toolkit (GATK), and the resulting variants were annotated with Annovar (Wang *et al.*, 2010). During variant prioritization, disease-causing variants reported in ClinVar (Landrum *et al.*, 2018) were given priority. Variants with a minor allele frequency <1% in the gnomAD and Iranome Databases, as well as intronic, intergenic, untranslated region, and synonymous variants with no effects on splice sites, were excluded. The pathogenicity of the remaining variants was predicted using SIFT (Ng and Henikoff, 2003), Polyphen-2 (Adzhubei *et al.*, 2013), CADD (Rentzsch *et al.*, 2019), Alpha Missense, REVEL (Ioannidis *et al.*, 2016), DANN (Quang *et al.*, 2015), and Mutation Taster. The candidate variant was classified according to the American College of Medical Genetics and Genomics (ACMG) guideline (Richards *et al.*, 2015).

Sanger sequencing and co-segregation study

Primer sequences were used as follows: F: 5'-GCCTTTGATGAGTCCCACGA and R: 5'-CCCTCCGAGACACTCCTACA (PCR product: 542 bp) for the *IGHMBP2* gene. PCR was conducted with an initial denaturation step at 95°C for 10 s, followed by 40 cycles of denaturation at 95°C for 30 sec., annealing at 60°C for 1 min, and extension at 72°C for 30 sec. To confirm the identified variant, after amplification, we performed Sanger sequencing on the patient and her family members using an ABI PRISM 3100 sequencer (Applied Biosystems, Foster City, CA, USA). Chromatograms were assessed using the Codon Code Aligner software.

Protein modeling and conservation analysis

To predict the effect of missense variants on the protein stability of *IGHMBP2*, we employed several prediction servers, including INPS-MD (Fariselli *et al.*, 2015), DDGemb (Savojardo *et al.*, 2024), mCSM (Pires *et al.*, 2020), DUET (Pires *et al.*, 2014), DDGun (Montanucci *et al.*, 2022), SDM (Worth *et al.*, 2011), DynaMut2 (Rodrigues *et al.*, 2021), and I-Mutant2.

Evolutionary conservation of *IGHMBP2* amino acids was assessed using the ConSurf (Ashkenazy *et al.*, 2016) and Clustal Omega online servers (Sievers and Higgins, 2014). Protein sequences from animal species-zebrafish (*Danio rerio*), chicken (*Gallus gallus*), mouse (*Mus musculus*), dog (*Canis lupus familiaris*), guinea pig (*Cavia porcellus*), and chimpanzee (*Pan troglodytes*), as well as the human species (*Homo sapiens*) -were acquired from the UniProt Database and uploaded to the Clustal Omega server (Sievers and Higgins, 2014). Protein conservation was analyzed using the ConSurf web server (Ashkenazy *et al.*, 2016), which estimates conservation based on phylogenetic relationships among homologous sequences. A three-dimensional structural model of the protein was generated using the AlphaFold server (<https://alphafold.ebi.ac.uk/>). Finally, structural effects of the wild-type and mutant proteins were compared using the Missense3D Database (Ittisoponpisan *et al.*, 2019) and visualized with ChimeraX.

Literature review and search method

Scientific databases, including PubMed and Scopus, were searched in English until August 2025. The search terms were combined with (CMT2S or Charcot Marie Tooth) and (*IGHMBP2*). The complete search strategy is provided in (Supplement 4). A total of 102 studies were screened, and 16 studies were selected. All studies were then imported into EndNote software. Studies were chosen for our literature review based on the following inclusion criteria: they contained both specified keywords: *IGHMBP2* and CMT2S. The exclusion criteria were (a) articles in languages other than English and (b) the title and abstract of any non-relevant studies. Following exclusion based on the mentioned criteria, a full-text version of all remaining articles was obtained and assessed. Finally, we analyzed the mutational spectrum, demographic data, and clinical features using Microsoft Excel. The flow chart of literature review screening is shown in Supplement 1.

Results

Clinical findings

In Figure 1, Patient V-1 (14 years old) was the first child of a first-degree consanguineous marriage. She had delayed gross motor

development and began walking at the age of two. She had previously undergone surgery for suspected clubfoot. At the age of seven, weakness of the distal hand muscles became evident, and her fine motor skills were impaired; for example, she had difficulty turning on a water tap. At the age of nine, she was referred to a pediatric neurologist because of progressive muscle weakness and atrophy involving both the upper and lower limbs, scoliosis, distal sensory and motor impairment, and areflexia. Electrophysiological testing was subsequently performed. Nerve conduction studies showed absent responses in motor nerves (tibial, deep peroneal nerve, median, and ulnar) and sensory nerves (sural, ulnar, median, and radial). Electromyography showed neurogenic findings. Brain and cervical spine MRI results were both normal. At the age of fourteen, she was re-evaluated and found to be severely impaired and wheelchair-bound. Spirometry assessment indicated normal respiratory function. Neither her parents nor siblings exhibited any symptoms related to the condition. Patient V-4 (Fig. 1), a four-year-old girl, presented with neuropathy and global developmental delay but no respiratory problems. Her parents showed no symptoms related to an *IGHMBP2*-related disorder.

Genetic testing findings

Whole-exome sequencing and bioinformatic analysis identified a novel homozygous missense variant, NM_002180: c.509T>C (p.Leu170Pro), in the *IGHMBP2* gene. The average coverage of exome sequencing was 107× (Supplement 3). Specifically, for the *IGHMBP2* gene, the mean depth of coverage was 114.71×, and the mean mapping quality (MAPQ) was 60. Sanger sequencing confirmed a heterozygous variant in both parents and a homozygous variant in the proband (Fig. 2A). This variant was also identified and confirmed in patient V-4 in homozygous form and in her parents, IV-19 and IV-20, in heterozygous form (Fig. 1).

In silico analysis of a variant

The identified variant was novel and had not been previously reported in the literature or in genetic databases such as ClinVar. Computational tools predicted a damaging impact on the protein. The variant was absent from population databases,

including gnomAD and Iranome. All prediction tools indicated a deleterious effect on protein function (Table 1). Protein stability prediction servers suggested that the variant destabilizes the protein structure (Table 2). Multiple sequence

alignments were performed using the Clustal Omega server across various species, revealing that the leucine at position 170 was conserved (**Error! Reference source not found.2B1**).

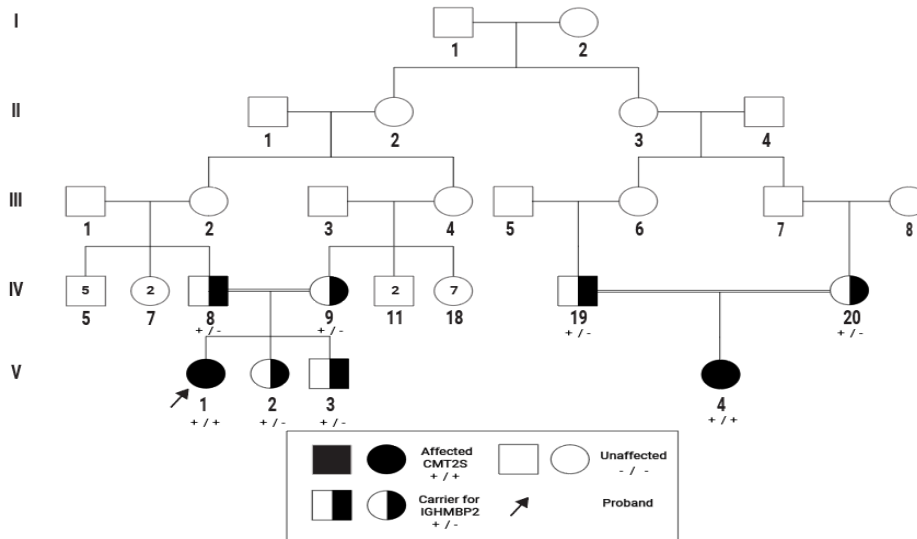


Fig. 1. The pedigree of Iranian first-cousin families affected by CMT2S, indicating heterozygous and homozygous states in unaffected and affected individuals, respectively.

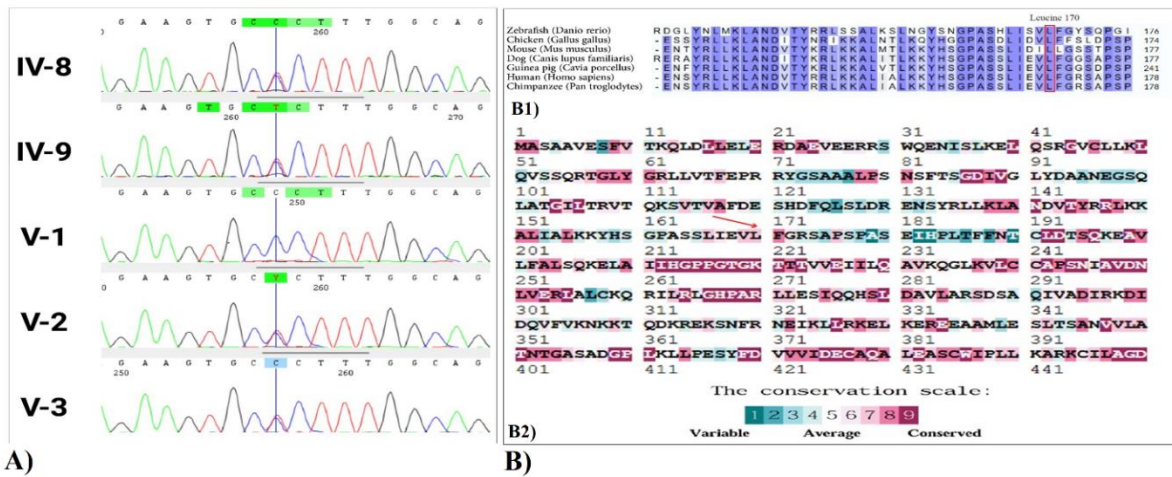


Fig. 2. Confirmation of detected variant: A) The chromatograms for the detected variant in the *IGHMBP2* gene in the family. Patient individual (V-1) is homozygote, while other members of the family are heterozygote; B1) Evolutionary conservation of Leucine170 as analyzed by the Clustal Omega web server; B2) Evolutionary conservation of Leucine170 as analyzed by the Consurf web server.

The Consurf evolutionary conservation score for leucine 170 was 7 (with a normalized score of -0.696), indicating that this buried amino acid is conserved and likely structurally significant (**Error! Reference source not found.2B2**). Subsequently, the *IGHMBP2* protein was

modeled using AlphaFold, with an average pLDDT score of 77.38 (high confidence). The pLDDT score for residue 170 was greater than 90 (very high confidence). Furthermore, the Missense3D database predicted that the leucine-to-proline substitution altered the secondary

structure of the protein from an 'H' (four-turn helix) to a 'T' (hydrogen-bonded turn), as shown in Fig. 3. After the screening review, 16 studies were included (Ahmed *et al.*, 2024; Cassini *et al.*, 2019; Chandrasekharan *et al.*, 2022; Cottenie *et al.*, 2014; Ipek *et al.*, 2025; Kulshrestha *et al.*, 2018; Lei *et al.*, 2022; Liu *et al.*, 2017; Liu *et al.*, 2024; Pedurupillay *et al.*, 2016; Schottmann *et al.*, 2015; Tkemaladze *et al.*, 2025; Tomaselli *et al.*, 2018; Tran *et al.*, 2024; Yavas *et al.*, 2025; Yuan *et al.*, 2017). 60 patients from 46 families were

reported with CMT2S. Together with the present case, 61 patients and 102 variants were initially identified (Supplement 2). However, Case 59 was excluded from both the clinical and the mutational spectrum analysis because only one heterozygous variant, c.734A>G p. (Asn245Ser), was reported. Therefore, the final analyzed cohort included 60 patients and 101 total variants, consisting of 59 previously reported patients and the present case (Supplement 7).

Table 1. Pathogenicity prediction and population frequency of novel variant in *IGHMBP2* gene

Web servers	SIFT	Polyphen 2	CADD	Alpha Missense	Revel	DANN
	D	D	25.1	likely pathogenic	D	D
Web servers	Mutation Taster	gnomAd V4.0.0	Iranome	ACMG classification	ACMG (evidence criteria)	-
	D	N/A	N/A	likely pathogenic	PM2, PP3_Moderate; PP1_Supporting; PP2_Supporting	-

D: deleterious; N/A: not applicable

Table 2. Protein stability prediction

INPS-MD	DDGemb	mCSM	DUET	DDGun	SDM	DynaMut2	I-mutant2
Destabilizing	Destabilizing	Destabilizing	Destabilizing	Destabilizing	Destabilizing	Destabilizing	Destabilizing

Demographic data

Among 60 patients with CMT2S (59 previously reported cases + 1 including case), 29 (48%) were male, and 31 (52%) were female (Supplement 7). The mean age of onset, available for 53 patients, was 3.40 years (SD± 3.83 years), with a median onset at two years. The interquartile range was 4.33 years, and the age of onset ranged from 40 days to 20 years (Supplement 7).

Mutational spectrum analysis

Before the analysis of the mutational spectrum, we reassessed 101 variants. In cases 6 and 38 (Supplement 7), two homozygous variants were reported for each individual. Variants c.861C>G and c.1363A>C were excluded due to their classification as benign and variant of uncertain significance (VUS), respectively. In case 30, three heterozygous variants were reported; the benign variant c.344C>T was excluded. As a result, only these three variants were excluded from variant counting, while the patients' clinical features remained included in the clinical analysis, resulting in a total of 98 variants. In contrast to case 59, which was excluded from both the

clinical analysis and variant counting, these patients (cases 6, 38, and 30) were retained in the clinical analysis because at least one disease-causing variant was reported for each patient. In the original studies, the additional variants were considered suspicious or potentially relevant at the time of publication; however, based on current knowledge and updated variant classification, variants that were not considered disease-causing were removed from the mutational spectrum analysis.

Among the 60 cases, 38 (63%) were compound heterozygous. The remaining 22 patients (36%) were homozygous. For variant type distribution, each heterozygous variant in compound heterozygous patients was counted separately, while homozygous variants were counted once per patient.

Among the 98 total variant occurrences, the most common variant type was nonsynonymous missense (49 variants, 50%), and followed by splicing (15 variants, 15.3%), frameshift (15 variants, 15.3%), nonsense (14 variants, 14.5%), large homozygous deletion (2 variants, 2%), start loss (1 variant, 1%), in-frame (1 variant, 1%), and intronic variants (1 variant, 1%) (Table 3).

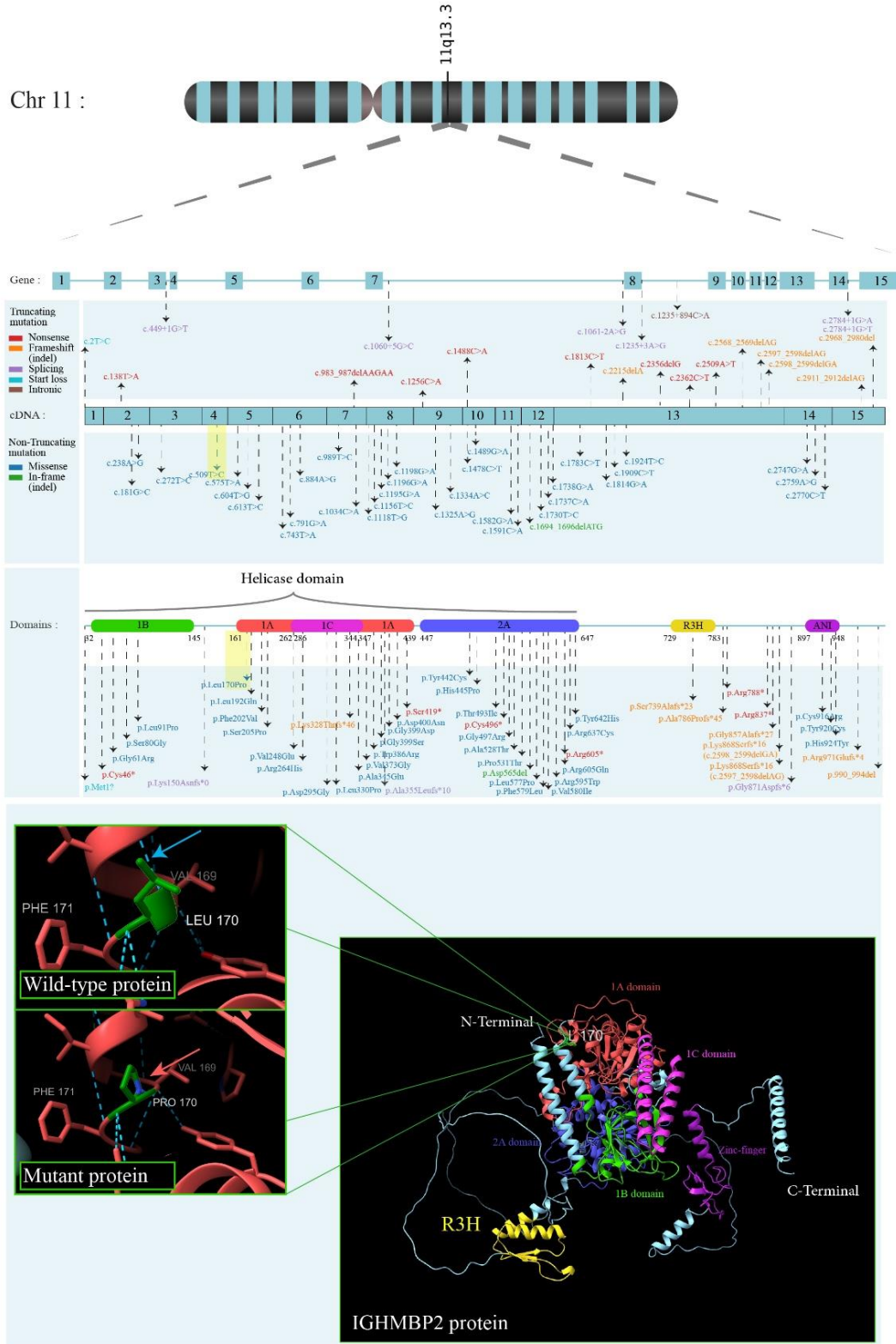


Fig. 3. Schematic representation of the *IGHMBP2* gene and protein structure. The variant identified in our study is highlighted with a yellow square. The upper and middle sections of the figure show CMT2S variants reported in the literature. The lower section of the figure displays the 3D protein model and the impact of the identified variant. The blue arrows and red arrows show the disruption of the hydrogen bond and alpha helix, respectively.

Variant distribution across *IGHMBP2* exons and introns is illustrated in Fig. 4, with exon 13 showing the highest frequency (17 variants). The most common variant was c.1235+3A>G (p. Ala355Leufs*10) in seven patients, followed by

c.138T>A (p. Cys46*) in six patients, and both c.1591C>A (p. Pro531Thr) and c.2911_2912delAG (p. Arg971Glufs*4) in five patients.

Table 3. Summary of clinical findings of CMT2S patients from our literature review

Gender	Muscle wasting (n/N)	Muscle weakness (n/N)	Absent or reduced reflexes (n/N)	Respiratory Support (n/N)	Gait disturbance (n/N)	Foot deformity* (n/N)	Scoliosis (n/N)
Male (n = 29)	UL: 16/22 LL: 21/22	UL: 25/ 28 LL: 29/29	24/25	3/29	16/25	20/26	5/26
Female (n = 31)	UL: 22/24 LL: 24/24	UL: 30/31 LL: 31/31	30/31	1/31	19/27	19/28	7/28

n= represents the number of patients exhibiting the clinical feature; N= represents the number of patients for whom information on that feature was available. Patients with missing or unreported data were excluded from the denominator; &= foot deformities and problems, including pes cavus, pes planus, foot valgus, club foot, pes equinus; UL= upper limb; LL= lower limb. Case 59 was excluded from the male group because only a heterozygous *IGHMBP2* variant was reported.

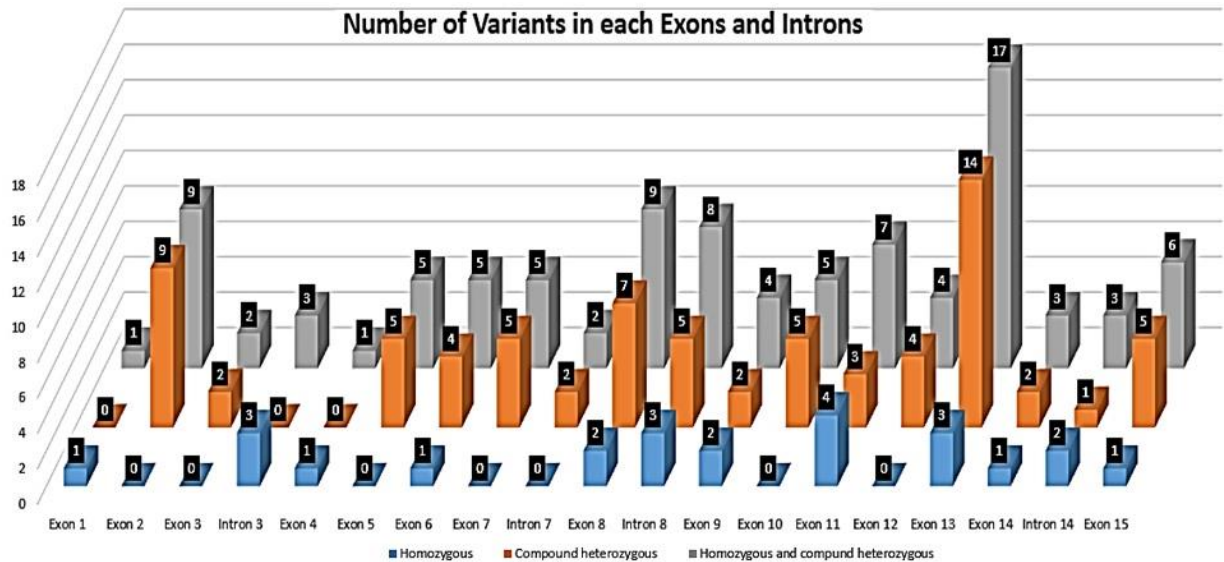


Fig. 4. Variant distribution across the exons and introns of the *IGHMBP2* gene in CMT2S cases. Large deletions are not shown.

Clinical features

Clinical data from 60 patients (59 previously reported cases+ 1 our case) are summarized in Table 3 (Ahmed *et al.*, 2024; Cassini *et al.*, 2019; Chandrasekharan *et al.*, 2022; Cottenie *et al.*, 2014; Ipek *et al.*, 2025; Kulshrestha *et al.*, 2018; Lei *et al.*, 2022; Liu *et al.*, 2017; Liu *et al.*, 2024; Pedurupillay *et al.*, 2016; Schottmann *et al.*, 2015; Tkemaladze *et al.*, 2025; Tomaselli *et al.*, 2018; Tran *et al.*, 2024; Yavas *et al.*, 2025; Yuan *et al.*, 2017). Among these patients, four (three males and one female) required ventilatory support due to late-onset respiratory involvement

(Kulshrestha *et al.*, 2018; Pedurupillay *et al.*, 2016; Schottmann *et al.*, 2015; Tomaselli *et al.*, 2018). Diaphragmatic weakness was documented in three affected males (Kulshrestha *et al.*, 2018; Pedurupillay *et al.*, 2016; Schottmann *et al.*, 2015). Autonomic dysfunction involving the gastrointestinal or urinary systems was reported in three cases, two males and one female (Pedurupillay *et al.*, 2016; Schottmann *et al.*, 2015). Creatine kinase levels were available for five patients; two had normal levels, while three demonstrated elevated levels (Ipek *et al.*, 2025; Tkemaladze *et al.*, 2025; Yavas *et al.*, 2025).

Discussion

In this study, we present a case of a 14-year-old girl from an Iranian consanguineous family diagnosed with CMT2S. A novel homozygous missense variant, c.509T>C p. (Leu170Pro), in the *IGHMBP2* gene was identified as the likely molecular cause of the disease. This variant was also confirmed in other family members in the heterozygous state by co-segregation analysis. Since this variant has not been previously reported in the literature and genetic databases, its pathogenicity and impact on protein stability were evaluated using bioinformatics tools and protein stability prediction servers.

The clinical presentation of the proband was compatible with previously reported cases of CMT2S. Her first manifestation was delayed gross motor development, with independent walking achieved at two years of age. This age is close to the median age of onset identified in our literature review, which reported a median of 2 years and a mean age of onset of 3.4 years. Furthermore, similar delays in motor milestones have been reported in other studies (Cottenie *et al.*, 2014; Schottmann *et al.*, 2015; Tran *et al.*, 2024; Yavas *et al.*, 2025). Other clinical features of our patient included muscle weakness and atrophy in all limbs, scoliosis, absent reflexes, EMG showing neurogenic changes, and absent motor and sensory nerves, which were compatible with CMT2S.

A clinically important feature in our patient was the absence of respiratory failure. Spirometry at the age of 14 years showed normal respiratory function, and the patient's V-4 also had no respiratory problems. This finding supports a diagnosis of CMT2S rather than SMARD1, in which early respiratory distress is a key feature. Although respiratory failure is uncommon in individuals with CMT2S, late-onset respiratory involvement has been reported in four cases (Kulshrestha *et al.*, 2018; Pedurupillay *et al.*, 2016; Schottmann *et al.*, 2015; Tomaselli *et al.*, 2018). One female patient required ventilation at age nine. Additionally, three male patients, aged 5, 9, and 15 years, developed diaphragmatic weakness requiring respiratory support. Other autonomic symptoms, including gastrointestinal and bladder dysfunction, excessive sweating, tachycardia, and constipation, have been

documented in three cases (Schottmann *et al.*, 2015; Tomaselli *et al.*, 2018). Scoliosis has also been documented in 12 patients: 5 males (Tran *et al.*, 2024; Liu *et al.*, 2024; Kulshrestha *et al.*, 2018; Schottmann *et al.*, 2015; Cottenie *et al.*, 2014) and 7 females (Liu *et al.*, 2024; Lei *et al.*, 2022; Tomaselli *et al.*, 2018; Schottmann *et al.*, 2015; Cottenie *et al.*, 2014).

In our mutational spectrum analysis, most of the patients had compound heterozygous variants. Missense variants were the most frequent variant type, accounting for 49 of 98 variants, followed by splicing, frameshift, and nonsense variants. Exon 13 also contained the highest number of variants related to CMT2S, followed by exons 2 and 8. The predominance of missense variants in CMT2S is relevant to the present case, which is also caused by a homozygous missense change. A clear genotype-phenotype correlation for *IGHMBP2* has not been established (Liu *et al.*, 2024). A previous systematic review suggested a possible association between *IGHMBP2* variant type, variant location, and clinical phenotype. The authors proposed that a combination of a nonsense variant in the 5' region with either a truncating or homozygous variant in the last exon may result in CMT2S because of residual protein function, whereas non-truncating variants within the two RecA-like domains were more frequently associated with SMARD1 (Tian *et al.*, 2023). However, this relationship was not presented as an absolute genotype-phenotype rule. In the present study, we identified a homozygous missense variant in the Rec1A subdomain associated with CMT2S rather than SMARD1. This finding may broaden the phenotypic spectrum associated with variants in the RecA-like domains and further supports the complexity of genotype-phenotype correlations in *IGHMBP2*-related disorders.

The identified homozygous variant, c.509T>C (p. Leu170Pro), is located in the helicase domain and affects a conserved residue at the end of an α -helix, introducing a buried proline. Protein stability analyses predict that this substitution disrupts the *IGHMBP2* structure, potentially reducing its stability and function. Specifically, the substitution of leucine with proline is predicted to disrupt both the hydrogen bonding and the α -helix (Fig. 3). According to ACMG guidelines, this variant is classified as likely

pathogenic and meets the PM2, PP3_Moderate, PP1_supporting, and PP2_supporting criteria, a justification for each criterion was discussed in Supplement 5 & 6 and Fig. 3. Further functional studies are needed to investigate the effect of p.

Leu170Pro. As of August 2025, 1,478 variants in the *IGHMBP2* gene were listed in ClinVar. Among these variants, 548 were VUS, representing the largest category (Fig. 5).

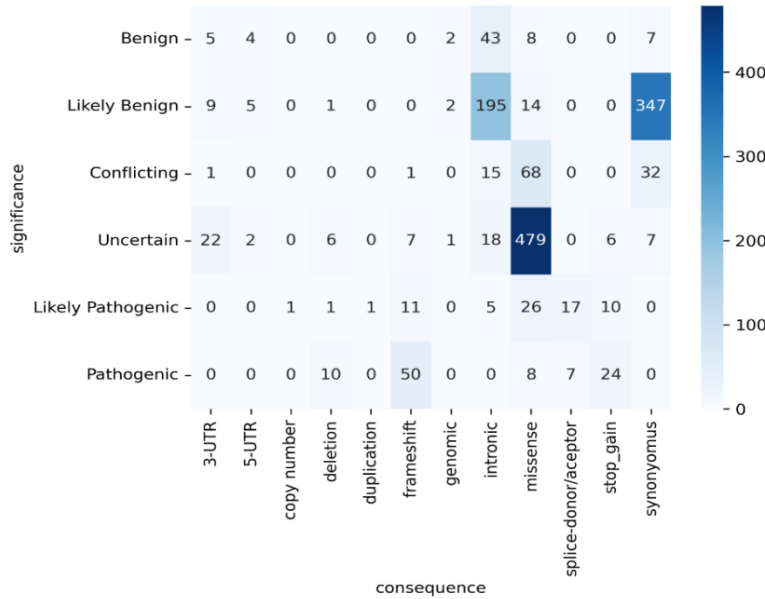


Fig. 5. Distribution of *IGHMBP2* variants in the ClinVar Database, classified by variant type and pathogenicity.

These findings indicate that the clinical impact of many *IGHMBP2* variants remains uncertain. Notably, there are 479 missense variants that are classified as VUS, and the correlations of many missense variants to phenotype are not well understood. As a result, missense variants with VUS classification require further functional, clinical, and *in silico* investigations. The present case contributes clinical and segregation evidence that may aid the interpretation of *IGHMBP2* missense variants, particularly those associated with CMT2S.

Several limitations should be acknowledged. First, although the identified *IGHMBP2* variant is predicted by *in silico* analyses to affect protein stability and structure, the mechanism by which this variant causes CMT2S rather than SMARD1 remains unknown. Additional functional studies and structural analyses are required to clarify the underlying disease mechanism. Second, our literature review was limited because we did not expand our search in other databases, including Embase and ScienceDirect, which may have introduced potential bias into our findings.

Therefore, a comprehensive systematic review in the future could improve our current knowledge of genotype-phenotype correlations in *IGHMBP2*-related disorders.

In conclusion, we identified a novel homozygous missense variant, c.509T>C (p.Leu170Pro), in a patient diagnosed with CMT2S. The observed clinical features, segregation pattern, absence from population databases, and *in silico* findings, including evolutionary conservation and protein structure analysis, indicate that the identified *IGHMBP2* variant is likely responsible for the disease.

Acknowledgement

We are grateful to the patient and their family for participating in this research. We also thank Dr. Ehsan Ghayoor Karmani and Dr. Mohammad Doosti from Next Generation Polyclinic, Dr. Mahya Hosseini from the Department of Pediatrics at Birjand University of Medical Sciences, and Dr. Shahriyar Shekani from the Pars Genetic Counseling Center for their valuable assistance in conducting this project.

Ethical consideration

This study was approved by the Ethics Committee of Tarbiat Modares University, Tehran, Iran (ethical code: IR.MODARES.REC.1404.015), in accordance with the principles of the Declaration of Helsinki. Written informed consent was obtained from both the patient and the legal representative for blood sampling and genetic analysis. Both the patient and the legal representative agreed to the publication of the article.

Conflict of interests

The authors declare no conflict of interest.

Data availability statement

The data supporting the findings of this study are available from the corresponding author upon reasonable request.

References

- Adzhubei, I., Jordan, D. M., & Sunyaev, S. R. (2013). Predicting functional effect of human missense mutations using PolyPhen-2. *Current Protocols in Human Genetics*, 76(1), 7-20. <https://doi.org/10.1002/0471142905.hg0720s76>
- Ahmed, A. N., Rawlins, L. E., Khan, N., Jan, Z., Ubeyratna, N., Voutsina, N., Azeem, A., Khan, S., Baple, E. L., Crosby, A. H., & Saleha, S. (2024). Expanding the genetic spectrum of hereditary motor sensory neuropathies in Pakistan. *BMC Neurology*, 24(1), 394. <https://doi.org/10.1186/s12883-024-03882-y>
- Ashkenazy, H., Abadi, S., Martz, E., Chay, O., Mayrose, I., Pupko, T., & Ben-Tal, N. (2016). ConSurf 2016: An improved methodology to estimate and visualize evolutionary conservation in macromolecules. *Nucleic Acids Research*, 44(W1), W344-350. <https://doi.org/10.1093/nar/gkw408>
- Bolger, A. M., Lohse, M., & Usadel, B. (2014). Trimmomatic: a flexible trimmer for Illumina sequence data. *Bioinformatics*, 30(15), 2114-2120. <https://doi.org/10.1093/bioinformatics/btu170>
- Cassini, T. A., Duncan, L., Rives, L. C., Newman, J. H., Phillips, J. A., Koziura, M. E., Brault, J., Hamid, R., Cogan, J., & Undiagnosed Diseases, N. (2019). Whole genome sequencing reveals novel *IGHMBP2* variant leading to unique cryptic splice-site and charcot-marie-tooth phenotype with early onset symptoms. *Molecular Genetics and Genomic Medicine*, 7(6), e00676. <https://doi.org/10.1002/mgg3.676>
- Chandrasekharan, S. V., Nair, S. S., Ganapathy, A., Mannan, A. U., & Sundaram, S. (2022). Charcot-marie-tooth disease type 2S: identical novel missense mutation of *IGHMBP2* gene in two unrelated families. *Neurological Sciences*, 43(1), 719-722. <https://doi.org/10.1007/s10072-021-05668-3>
- Cottenie, E., Kochanski, A., Jordanova, A., Bansagi, B., Zimon, M., Horga, A., Jaunmuktane, Z., Saveri, P., Rasic, V. M., Baets, J., Bartsakoulia, M., Ploski, R., Teterycz, P., Nikolic, M., Quinlivan, R., Laura, M., Sweeney, M. G., Taroni, F., Lunn, M. P., Houlden, H. (2014). Truncating and missense mutations in *IGHMBP2* cause Charcot-Marie Tooth disease type 2. *American Journal of Human Genetics*, 95(5), 590-601. <https://doi.org/10.1016/j.ajhg.2014.10.002>
- De Planell-Saguer, M., Schroeder, D. G., Rodicio, M. C., Cox, G. A., & Mourelatos, Z. (2009). Biochemical and genetic evidence for a role of *IGHMBP2* in the translational machinery. *Human Molecular Genetics*, 18(12), 2115-2126. <https://doi.org/10.1093/hmg/ddp134>
- Fariselli, P., Martelli, P. L., Savojardo, C., & Casadio, R. (2015). INPS: Predicting the impact of non-synonymous variations on protein stability from sequence. *Bioinformatics*, 31(17), 2816-2821. <https://doi.org/10.1093/bioinformatics/btv291>
- Ioannidis, N. M., Rothstein, J. H., Pejaver, V., Middha, S., McDonnell, S. K., Baheti, S., Musolf, A., Li, Q., Holzinger, E., Karyadi, D., Cannon-Albright, L. A., Teerlink, C. C., Stanford, J. L., Isaacs, W. B., Xu, J., Cooney, K. A., Lange, E. M., Schleutker, J., Carpten, J. D., Sieh, W. (2016). REVEL: An ensemble method for predicting the pathogenicity of rare missense variants. *American Journal of Human Genetics*, 99(4), 877-885. <https://doi.org/10.1016/j.ajhg.2016.08.016>
- Ipek, R., Cavdartepe, B. E., Bozdogan, S. T., Altunisik, E., Akalin, A., Yaman, M., Akin, A., & Kumandas, S. (2025). Genotypic and phenotypic characterization of axonal charcot-

- marie-tooth disease in childhood: Identification of one novel and four known mutations. *Genes*, 16(8), 917. <https://doi.org/10.3390/genes16080917>
- Ittisoponpisan, S., Islam, S. A., Khanna, T., Alhuzimi, E., David, A., & Sternberg, M. J. E. (2019). Can predicted protein 3D structures provide reliable insights into whether Missense variants are disease Associated? *Journal of Molecular Biology*, 431(11), 2197-2212. <https://doi.org/10.1016/j.jmb.2019.04.009>
- Kanaan, J., Raj, S., Decourty, L., Saveanu, C., Croquette, V., & Le Hir, H. (2018). UPF1-like helicase grip on nucleic acids dictates processivity. *Nature Communications*, 9(1), 3752. <https://doi.org/10.1038/s41467-018-06313-y>
- Kulshrestha, R., Forrester, N., Antoniadi, T., Willis, T., Sethuraman, S. K., & Samuels, M. (2018). Charcot marie tooth disease type 2S with late onset diaphragmatic weakness: An atypical case. *Neuromuscular Disorders: NMD*, 28(12), 1016-1021. <https://doi.org/10.1016/j.nmd.2018.09.008>
- Landrum, M. J., Lee, J. M., Benson, M., Brown, G. R., Chao, C., Chitipiralla, S., Gu, B., Hart, J., Hoffman, D., Jang, W., Karapetyan, K., Katz, K., Liu, C., Maddipatla, Z., Malheiro, A., McDaniel, K., Ovetsky, M., Riley, G., Zhou, G., Maglott, D. R. (2018). ClinVar: Improving access to variant interpretations and supporting evidence. *Nucleic Acids Research*, 46(D1), D1062-D1067. <https://doi.org/10.1093/nar/gkx1153>
- Lau, A. M., Bordin, N., Kandathil, S. M., Sillitoe, I., Waman, V. P., Wells, J., Orengo, C. A., & Jones, D. T. (2024). Exploring structural diversity across the protein universe with The Encyclopedia of domains. *Science*, 386(6721), eadq4946. <https://doi.org/10.1126/science.adq4946>
- Lei, L., Zhiqiang, L., Xiaobo, L., Zhengmao, H., Shunxiang, H., Huadong, Z., Beisha, T., & Ruxu, Z. (2022). Clinical and genetic features of charcot-marie-tooth disease patients with *IGHMBP2* mutations. *Neuromuscular Disorders: NMD*, 32(7), 564-571. <https://doi.org/10.1016/j.nmd.2022.05.002>
- Lim, S. C., Bowler, M. W., Lai, T. F., & Song, H. (2012). The *IGHMBP2* helicase structure reveals the molecular basis for disease-causing mutations in DMSA1. *Nucleic Acids Research*, 40(21), 11009-11022. <https://doi.org/10.1093/nar/gks792>
- Liu, L., Li, X., Hu, Z., Mao, X., Zi, X., Xia, K., Tang, B., & Zhang, R. (2017). *IGHMBP2*-related clinical and genetic features in a cohort of Chinese charcot-marie-tooth disease type 2 patients. *Neuromuscular Disorders: NMD*, 27(2), 193-199. <https://doi.org/10.1016/j.nmd.2016.11.008>
- Liu, L., Zeng, S., Li, X., Xie, Y., Xu, K., Yang, H., Huang, S., Zhao, H., & Zhang, R. (2024). Genotype-phenotype correlations of AR-CMT2S in a cohort of axonal charcot-marie-tooth patients from central south china. *Journal of the Peripheral Nervous System*, 29(2), 243-251. <https://doi.org/10.1111/jns.12633>
- Montanucci, L., Capriotti, E., Birolo, G., Benevenuta, S., Pancotti, C., Lal, D., & Fariselli, P. (2022). DDGun: An untrained predictor of protein stability changes upon amino acid variants. *Nucleic Acids Reserch*, 50(W1), W222-W227. <https://doi.org/10.1093/nar/gkac325>
- Ng, P. C., & Henikoff, S. (2003). SIFT: Predicting amino acid changes that affect protein function. *Nucleic Acids Research*, 31(13), 3812-3814. <https://doi.org/10.1093/nar/gkg509>
- Park, J., Desai, H., Liboy-Lugo, J. M., Gu, S., Jowhar, Z., Xu, A., & Floor, S. N. (2024). *IGHMBP2* deletion suppresses translation and activates the integrated stress response. *Life Science Alliance*, 7(8). <https://doi.org/10.26508/lsa.202302554>
- Pedurupillay, C. R., Amundsen, S. S., Baroy, T., Rasmussen, M., Blomhoff, A., Stadheim, B. F., Orstavik, K., Holmgren, A., Iqbal, T., Frengen, E., Misceo, D., & Stromme, P. (2016). Clinical and molecular characteristics in three families with biallelic mutations in *IGHMBP2*. *Neuromuscular Disorders*, 26(9), 570-575. <https://doi.org/10.1016/j.nmd.2016.06.457>
- Pires, D. E., Ascher, D. B., & Blundell, T. L. (2014). DUET: A server for predicting effects of mutations on protein stability using an integrated computational approach. *Nucleic Acids Research*, 42(Web Server issue), W314-319. <https://doi.org/10.1093/nar/gku411>

- Pires, D. E. V., Rodrigues, C. H. M., & Ascher, D. B. (2020). mCSM-membrane: Predicting the effects of mutations on transmembrane proteins. *Nucleic Acids Research*, 48(W1), W147-W153. <https://doi.org/10.1093/nar/gkaa416>
- Prusty, A. B., Hirmer, A., Sierra-Delgado, J. A., Huber, H., Guenther, U. P., Schlosser, A., Dybkov, O., Yildirim, E., Urlaub, H., Meyer, K. C., Jablonka, S., Erhard, F., & Fischer, U. (2024). RNA helicase *IGHMBP2* regulates THO complex to ensure cellular mRNA homeostasis. *Cell Report*, 43(2), 113802. <https://doi.org/10.1016/j.celrep.2024.113802>
- Quang, D., Chen, Y., & Xie, X. (2015). DANN: A deep learning approach for annotating the pathogenicity of genetic variants. *Bioinformatics*, 31(5), 761-763. <https://doi.org/10.1093/bioinformatics/btu703>
- Rentzsch, P., Witten, D., Cooper, G. M., Shendure, J., & Kircher, M. (2019). CADD: Predicting the deleteriousness of variants throughout the human genome. *Nucleic Acids Research*, 47(D1), D886-D894. <https://doi.org/10.1093/nar/gky1016>
- Richards, S., Aziz, N., Bale, S., Bick, D., Das, S., Gastier-Foster, J., Grody, W. W., Hegde, M., Lyon, E., Spector, E., Voelkerding, K., Reh, H. L., & Committee, A. L. Q. A. (2015). Standards and guidelines for the interpretation of sequence variants: a joint consensus recommendation of the American College of Medical Genetics and Genomics and the Association for Molecular Pathology. *Genetics in Medicine*, 17(5), 405-424. <https://doi.org/10.1038/gim.2015.30>
- Rodrigues, C. H. M., Pires, D. E. V., & Ascher, D. B. (2021). DynaMut2: Assessing changes in stability and flexibility upon single and multiple point missense mutations. *Protein Science*, 30(1), 60-69. <https://doi.org/10.1002/pro.3942>
- Rzepnikowska, W., Kaminska, J., & Kochanski, A. (2024). The molecular mechanisms that underlie *IGHMBP2*-related diseases. *Neuropathology and Applied Neurobiology*, 50(4), e13005. <https://doi.org/10.1111/nan.13005>
- Rzepnikowska, W., & Kochanski, A. (2021). Models for *IGHMBP2*-associated diseases: An overview and a roadmap for the future. *Neuromuscular Disorders*, 31(12), 1266-1278. <https://doi.org/10.1016/j.nmd.2021.08.001>
- Savojardo, C., Manfredi, M., Martelli, P. L., & Casadio, R. (2024). DDGemb: Predicting protein stability change upon single and multipoint variations with embeddings and deep learning. *Bioinformatics*, 41(1). <https://doi.org/10.1093/bioinformatics/btaf019>
- Schottmann, G., Jungbluth, H., Schara, U., Knierim, E., Morales Gonzalez, S., Gill, E., Seifert, F., Norwood, F., Deshpande, C., von Au, K., Schuelke, M., & Senderek, J. (2015). Recessive truncating *IGHMBP2* mutations presenting as axonal sensorimotor neuropathy. *Neurology*, 84(5), 523-531. <https://doi.org/10.1212/WNL.0000000000001220>
- Sievers, F., & Higgins, D. G. (2014). Clustal omega, accurate alignment of very large numbers of sequences. *Methods in Molecular Biology*, 1079, 105-116. <https://doi.org/10.1007/978-1-62703-646-7-6>
- Tian, Y., Xing, J., Shi, Y., & Yuan, E. (2023). Exploring the relationship between *IGHMBP2* gene mutations and spinal muscular atrophy with respiratory distress type 1 and charcot-marie-tooth disease type 2S: a systematic review. *Frontiers in Neuroscience*, 1252075. <https://doi.org/10.3389/fnins.2023.1252075>
- Tkemaladze, T., Bregvadze, K., Abashishvili, L., Chikvinidze, G., Delgado Vega, A. M., Akbar, F., Khan, S., & Kirmani, S. (2025). Clinical and genetic landscape of *IGHMBP2* related disorders: From novel variants to phenotypic insights. *American Journal of Medical Genetics*, 197(9), e64116. <https://doi.org/10.1002/ajmg.a.64116>
- Tomaselli, P. J., Horga, A., Rossor, A. M., Jaunmuktane, Z., Cortese, A., Blake, J. C., Zarate-Lopez, N., Houlden, H., & Reilly, M. M. (2018). *IGHMBP2* mutation associated with organ-specific autonomic dysfunction. *Neuromuscular Disorders*, 28(12), 1012-1015. <https://doi.org/10.1016/j.nmd.2018.08.010>
- Tran, V. K., Cao, M. H., Nguyen, T. T. H., Le, P. T., Tran, H. A., Vu, D. C., Nguyen, H. T., Nguyen, M. T. P., Bui, T. H., Nguyen, T. B., Ta, T. V., & Tran, T. H. (2024). A novel *IGHMBP2* variant and clinical diversity in vietnamese SMARD1 and CMT2S patients. *Frontiers in Pediatrics*, 12, 1165492. <https://doi.org/10.3389/fped.2024.1165492>

- Wang, K., Li, M., & Hakonarson, H. (2010). ANNOVAR: Functional annotation of genetic variants from high-throughput sequencing data. *Nucleic Acids Research*, 38(16), e164. <https://doi.org/10.1093/nar/gkq603>
- Worth, C. L., Preissner, R., & Blundell, T. L. (2011). SDM: A server for predicting effects of mutations on protein stability and malfunction. *Nucleic Acids Research*, 39, W215-222. <https://doi.org/10.1093/nar/gkr363>
- Yavas, C., Dogan, M., Ozgor, B., Akbulut, E., & Eroz, R. (2025). Novel biallelic nonsense mutation in *IGHMBP2* gene linked to neuropathy (CMT2S): A comprehensive clinical, genetic and bioinformatic analysis of a Turkish patient with literature review. *Brain and Development*, 47(1), 104313. <https://doi.org/10.1016/j.braindev.2024.104313>
- Yuan, J. H., Hashiguchi, A., Yoshimura, A., Yaguchi, H., Tsuzaki, K., Ikeda, A., Wada-Isoe, K., Ando, M., Nakamura, T., Higuchi, Y., Hiramatsu, Y., Okamoto, Y., & Takashima, H. (2017). Clinical diversity caused by novel *IGHMBP2* variants. *Journal of Human Genetics*, 62(6), 599-604. <https://doi.org/10.1038/jhg.2017.15>